

Control of coupled oscillator networks

Per Sebastian Skardal and Alex Arenas

Department d'Enginyeria Informàtica i Matemàtiques, Universitat Rovira i Virgili,
Tarragona, Spain

Abstract

The control of complex systems and network-coupled dynamical systems is a topic of vital theoretical importance in mathematics and physics with a wide range of applications in engineering and various other sciences. Here we consider the important case of networks of coupled phase oscillators with nonlinear interactions—a paradigmatic example that has guided our understanding of synchronization for decades. We develop a method for control based on identifying and stabilizing problematic oscillators, resulting in a stable spectrum of eigenvalues, and in turn a linearly stable synchronized state. Interestingly, the amount of control, i.e., number of oscillators, required to stabilize the network is primarily dictated by the coupling strength, dynamical heterogeneity, and mean degree of the network, and depends little on the structural heterogeneity of the network itself.

Complex networks and complex systems describe the physical, biological, and social structures that connect our world and host the dynamical processes vital to our lives [1, 2, 3]. The failure of such large-scale systems to operate in the desired way can thus lead to catastrophic events such as power outages [4, 5], extinctions [6, 7], and economic collapses [8, 9]. Thus, the development and design of efficient and effective control mechanisms for such systems is not only a question of theoretical interest to mathematicians, but has a wide range of important applications in physics, chemistry, biology, engineering, and the social sciences [10].

In recent years the topic of control of complex networks and complex systems has exploded. Based on the paradigm of linear homogenous dynamical systems, pioneering works have led to the development of the concept of *controllability* of complex networks [11, 12] and has enabled further advances related to controllability such as centrality [13], energy [14], effect of correlations [15], emergence of bimodality [16], transtion and nonlocality [17], the specific role of individual nodes [18], target control [19], and control of edges in switchboard dynamics [20]. While these works shed much light on the connection between control and network structure, other vital works have addressed the control of networks of nonlinear dynamical systems using compensatory perturbations [21, 22] and pinning techniques [23, 24, 25].

Here we develop a control mechanism for networks of coupled phase oscillators. Our goal is to induce a synchronized state and guarantee asymptotic stability by applying as few control gains to the network as possible. Our method is based on finding the Jacobian of the desired synchronized state and studying its spectrum, by which we identify the oscillators in the network that contribute to unstable eigenvalues and thus destabilize the synchronized state. Importantly, our method not only identifies which oscillators require control, but also the required strength of each control gain. The problem we address here combines many challenges at once, namely, dynamical nonlinearity and both dynamical and structural heterogeneity. Interestingly, we find that the control required to stabilize a network is dictated by the coupling strength, dynamical heterogeneity, and mean degree of the network, and depends little on the structural heterogeneity of the network. We conclude by discussing how our findings fit in a broader context and suggesting potential applications and future work. In addition to cardiac arrhythmias [26] and pathological brain dynamics [27] for which control techniques that promote synchronization could prove useful for developing treatments, we point to control techniques for stabilizing power grids [28, 29], in particular microgrids—small power networks whose dynamics have been proven to be described by Kuramoto oscillator networks [30].

Results

The Kuramoto model

We consider the famous Kuramoto model for the entrainment of many coupled dissipative oscillators [31]. The Kuramoto model consists of N phase oscillators θ_i for $i = 1, \dots, N$ that, when placed on a network dictating their pair-wise interactions, evolve according to

$$\dot{\theta}_i = \omega_i + K \sum_{j=1}^N A_{ij} \sin(\theta_j - \theta_i). \quad (1)$$

Each oscillator i has a unique natural frequency ω_i that describes its preferred angular velocity in the absence of interactions, which is often drawn randomly from a distribution $g(\omega)$. Furthermore, the global coupling strength K describes the influence that oscillators have on one another via the network connectivity, which is encoded in the adjacency matrix $[A_{ij}]$. Here we focus on the simple case of an undirected, unweighted network, but note that all results below generalize to directed and weighted networks. We also assume that the network is connected, i.e., irreducible. Over the last few decades the Kuramoto model has proven to be very useful for modeling real-world systems [32, 33], uncovering the mechanisms behind emergent collective behavior [34, 35], exploring additional effects such as time-delays [36] and community structure [37], and finding optimal networks structure [38].

Depending on the coupling strength K , as well as the frequency vector $\boldsymbol{\omega}$ and the network topology, the steady-state dynamics of Equation (1) can attain many different states that included com-

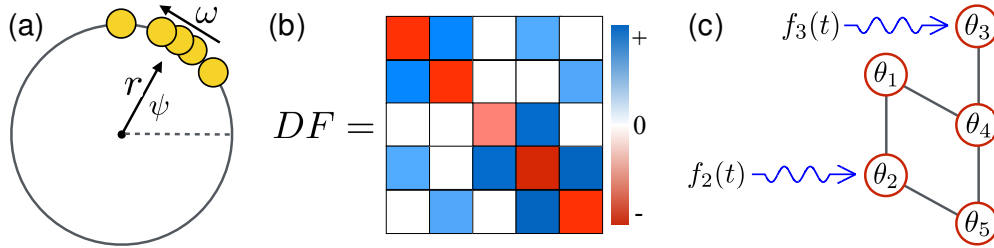


Figure 1: **Control of coupled oscillator networks.** For a five-oscillator network, illustration of (a) control applied to oscillators $i = 2$ and 3 , (b) the fully synchronized state, and (c) the Jacobian of a stable solution.

plete incoherence, partial synchronization, and full synchronization. The latter is characterized by $\lim_{t \rightarrow \infty} |\dot{\theta}_j(t) - \dot{\theta}_i(t)| = 0$ and is also referred to as full phase-locking or frequency-synchronization. The fully synchronized state (henceforth called the synchronized state) typically displays a large degree of phase synchronization $r \approx 1$, where $re^{i\psi} = N^{-1} \sum_{j=1}^N e^{i\theta_j}$ is that standard Kuramoto order parameter. In Figure 1(a) we illustrate a synchronized state in a group of five oscillators, each moving with an angular velocity of ω . The order parameter is illustrated as vector of length r with an offset angle ψ from the positive real axis.

Stability and control

In this Article we address the problem of control by first assuming that due to the system parameters (i.e., the coupling strength, natural frequency sequence, or network topology), the steady-state dynamics of Equation (1) are not synchronized, i.e., one or more oscillators remains desynchronized. Thus, our goal is to find a synchronized state and stabilize it. A straight-forward analysis shows that the synchronized state (within the rotating reference frame $\theta \mapsto \theta + \langle \omega \rangle t$) is given by the vector $\boldsymbol{\theta}^* = K^{-1} L^\dagger \boldsymbol{\omega}$, where L is the network Laplacian, $L_{ij} = \delta_{ij} \sum_l A_{il} - A_{ij}$, and L^\dagger is its pseudo-inverse [39]. We summarize a derivation of this result in the Methods. The stability of $\boldsymbol{\theta}^*$ is dictated by the Jacobian matrix whose entries are defined $[DF]_{ij} = \partial \dot{\theta}_i / \partial \theta_j$, and is stable if all the eigenvalues of $DF|_{\boldsymbol{\theta}^*}$ are non-positive. In our case we have that

$$DF_{ij} = \begin{cases} -K \sum_{j \neq i} A_{ij} \cos(\theta_j^* - \theta_i^*) & \text{if } i = j \\ KA_{ij} \cos(\theta_j^* - \theta_i^*) & \text{otherwise.} \end{cases} \quad (2)$$

We note that each row of DF sums to zero, i.e., satisfies $DF_{ii} = -\sum_{j \neq i} DF_{ij}$. This is a particularly convenient property for using the Gershgorin circle theorem [40], which implies that eigenvalues of DF lie within the union of closed discs D_i for $i = 1, \dots, N$, which are each centered at DF_{ii} and have radius R_i , where $R_i = \sum_{j \neq i} |DF_{ij}|$. (The full theorem is given in the Methods.) In particular, if all the off-diagonal entries of DF are non-negative, then each Gershgorin disc is contained in the left-half plane, implying that all eigenvalues are non-positive and the solution

is stable. An illustration of this case is presented in Figure 1(b). If, however, one or more non-diagonal entries of DF are negative, then each Gershgorin disc corresponding to a row with a negative off-diagonal entry enters the right-half plane, admitting the possibility for one or more positive eigenvalues and thus destabilization. Thus, the oscillators that require control can be easily identified as those whose corresponding rows have one or more negative off-diagonal entries.

We aim to stabilize the synchronized solution by adding one or more control gains to the system, as illustrated in Figure 1(c). We will refer to oscillators to which we apply control as *driver nodes*, and to oscillators to which we do not apply control as *free nodes*. We choose the control gains to take the form $f_i(t) = F_i \sin(\phi_i - \theta_i)$, where F_i is the strength of the i^{th} control gain and ϕ_i is a target phase that can in principle depend on either local or global information, and vary in time. Here we focus on the choice of target phase $\phi_i = \theta_i^*$, and discuss other possibilities below. Since the control gain depends on the current state of the system, this can be thought of as a form of feedback control. The new dynamics are then given by

$$\dot{\theta}_i = \omega_i + K \sum_{j=1}^N A_{ij} \sin(\theta_j - \theta_i) + F_i \sin(\theta_i^* - \theta_i), \quad (3)$$

where we take $F_i = 0$ for free nodes. While the off-diagonal entries of DF remain unaltered, the new diagonal entries are given by $DF_{ii} = -K \sum_{j \neq i} A_{ij} \cos(\theta_j^* - \theta_i^*) - F_i$. Thus, we set coupling gain strength of each driver node i such that it satisfies $F_i \geq K \sum_{j \neq i} A_{ij} [|\cos(\theta_j^* - \theta_i^*)| - \cos(\theta_j^* - \theta_i^*)]$. This ensures that all Gershgorin discs are contained in the left-half plane, implying that all eigenvalues are non-positive and the synchronized state is stable.

We now briefly comment on the choice of target phases ϕ_i in the control gains. In the method outlined above, we have set the target phase equal to the steady-state phase, $\phi_i = \theta_i^*$. This is a convenient choice for the derivation described above. Additionally, we find that in practice other choices also yield positive results. In particular, one choice that tends to yield slightly better results is to force each driver node towards the center of the synchronized cluster, i.e., $\phi_i = \bar{\phi}$, where we assume the cluster is centered at the angle $\bar{\phi}$. Target phases can also be chosen according to global or distributed control strategies. In particular, given the standard Kuramoto order parameter $re^{i\psi} = \sum_j e^{i\theta_j}/N$ or the set of local order parameters $r_i e^{i\psi_i} = \sum_j A_{ij} e^{i\theta_j}$, the choices $\phi_i = \psi$ and $\phi_i = \psi_i$ correspond to global and distributed control strategies that typically yield favorable results. We also note before presenting examples that since the method outlined above depends on the approximation of the steady-state solution $\theta^* \approx K^{-1}L^\dagger \omega$, in practice we add a buffer margin when identifying unstable oscillators, looking for non-diagonal entries of DF that are not necessarily negative, but rather less than some $\epsilon > 0$. We find that the choice $\epsilon = 0.2$ is sufficient, and is what we use in the examples below.

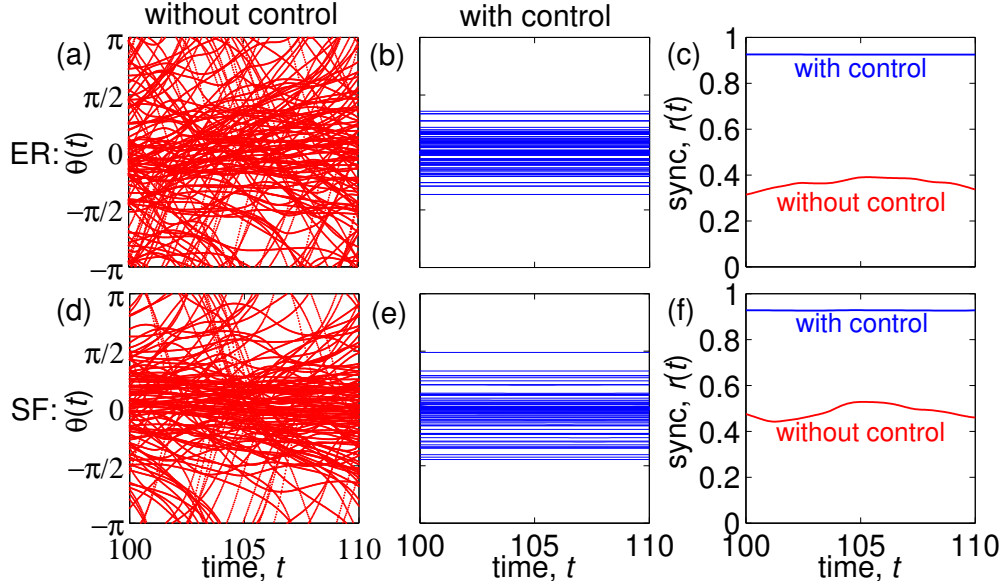


Figure 2: **Control of coupled oscillator networks: random networks.** Example of control applied to a coupled oscillator network with ER and SF topologies (top and bottom rows, respectively) with $\langle k \rangle = 6$ and $N = 1000$. The coupling strength is $K = 0.4$. Time series for phases $\theta_i(t)$ of 10% of oscillators (a), (d) without and (b), (e) with control. Driver nodes constituted 37.1% and 44.5% of the ER and SF networks, respectively. (c), (f) Time series for the degree of phase synchronization $r(t)$ for the networks without (red) and with (blue) control.

Control of random networks

We now demonstrate our approach by considering two types of random networks: Erdős-Rényi [41] (ER) networks and scale-free (SF) networks. Each ER network is constructed using a fixed link probability p and each SF network is built using the configuration model [42] with a degree sequence drawn from the distribution $P(k) \propto k^{-\gamma}$ with $\gamma = 3$ and enforced minimum degree k_0 . To tune the mean degree $\langle k \rangle$ of each network we set either $p = \langle k \rangle / (N - 1)$ or $k_0 = \langle k \rangle / (\gamma - 1)$. Figure 2 illustrates our results with an example of each type of network, where we have used networks of size $N = 1000$ with mean degree $\langle k \rangle = 6$, set the coupling strength $K = 0.4$, and used natural frequencies drawn from a uniform distribution with zero mean and unit variance. The top and bottom rows display the results for the ER and SF networks, respectively, displaying the time series $\theta(t)$ of 10% of the oscillators without control [first column, panels (a) and (d)] and with control [middle column, panels (b) and (e)], displayed after a long transient. The difference between no control to control is quite drastic, with a large fraction of desynchronized oscillators without control, and full synchronization with control. Driver nodes constituted 37.1% and 44.5% of the ER and SF networks, respectively, to attain the synchronized state. In the last column [panels (c) and (f)] we present the degree of phase synchronization, plotting the order parameter $r(t)$ for both solutions

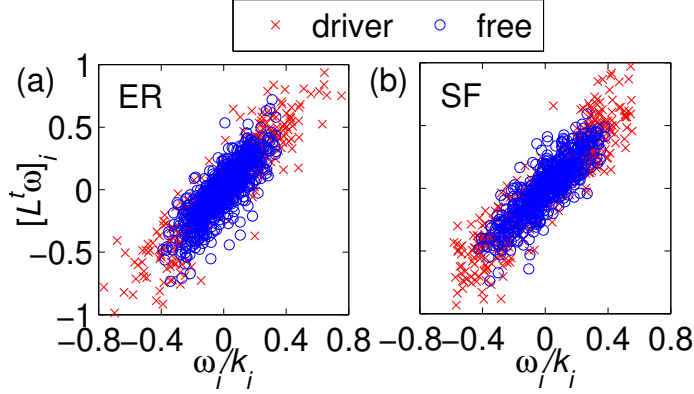


Figure 3: **Driver and free nodes.** $[L^\dagger\omega]_i$ vs ω_i/k_i for driver (red crosses) and free (blue circles) nodes in the (a) ER and (b) SF networks used in Figure 2.

with and without control. Unlike the solution without control, which fluctuates significantly at a relative low value, the solution with control reaches a steady value near $r(t) \approx 1$.

Next we investigate the properties of driver and free nodes by revisiting our method. This is an essential question due to the heterogeneity of the oscillators both in terms of network structure and also local dynamics (i.e., natural frequencies). An oscillator i is a driver node if one of its off-diagonal entries $DF_{ij} \propto \cos(\theta_j^* - \theta_i^*)$ is negative, and therefore oscillators with large (small) steady-state values $\theta_i^* \propto |[L^\dagger\omega]_i|$ tend to be driver (free) nodes. Furthermore, we find that these values scale approximately linearly with the ratio of the natural frequencies to degrees, i.e., $[L^\dagger\omega]_i \propto \omega_i/k_i$. We illustrate this in Figure 3, where we plot the relationship $[L^\dagger\omega]_i$ vs ω_i/k_i for the example ER and SF networks presented above [panels (a) and (b), respectively], denoting driver nodes with red crosses and free nodes with blue circles. These results show the important role that dynamics, in addition to network structure, plays in dictating controlling the system. In particular, driver nodes of the system tend to balance a large ratio (in absolute value) of natural frequencies to degrees.

Finally, we quantify the overall control require for synchronization by studying how the fraction of driver nodes, denoted $n_D = N_D/N$, where N_D is the total number of driver nodes, depends on both the system's dynamical and structural parameters. Presenting our results in Figure 4, we first explore how the fraction of driver nodes depends on the coupling strength by plotting in panel (a) n_D vs K for both ER and SF networks with mean degrees $\langle k \rangle = 4, 8, \text{ and } 12$ (blue circles, red triangles, and green squares, respectively). Results for ER and SF networks are plotted with unfilled and filled symbols, respectively, and each curve represents an average over 100 network realizations, each averaged over 100 random natural frequency realizations. While it is expected that n_D decreases monotonically with K , the curves' dependence on network topology and mean degree is nontrivial. In particular, the the shape of n_D vs K depends more sensitively on the mean degree than the topology, suggesting that network heterogeneity has little effect on overall control in comparison to average connectivity. In light of the significant dependence of overall control on

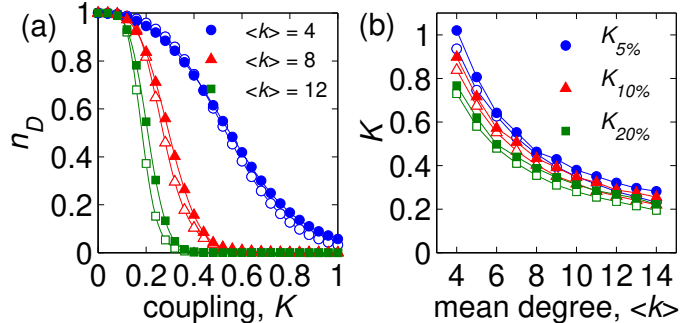


Figure 4: **Fraction of driver nodes.** (a) The fraction of driver nodes n_D in ER (unfilled symbols) and SF (filled symbols) as a function of coupling strength K for mean degrees $\langle k \rangle = 4, 8,$ and 12 (blue circles, red triangle, and green squares, respectively). (b) The required coupling strengths $K_{5\%}, K_{10\%},$ and $K_{20\%}$ required to achieve full phase synchronization given $n_D = 0.05, 0.1,$ and 0.2 . Each data point is the average over 100 network realizations of size $N = 1000,$ each averaged over 100 natural frequency realizations.

the coupling strength, we investigate the coupling strength required to synchronize a network if limited amount of control is available. To this end we calculate for each family of networks the required coupling strengths $K_{5\%}, K_{10\%},$ and $K_{20\%}$ for which, on average, a fraction $n_D = 0.05, 0.1,$ and 0.2 will achieve synchronization as a function of the average degree $\langle k \rangle$. We plot the results in Figure 4 (b). We point out again that ER and SF networks behave very similarly on average, and that with a larger mean degree, a smaller coupling strength is required to achieve synchronization.

Discussion

Theoretical and practical aspects of the control of dynamical processes remains an important and ongoing area of interdisciplinary research at the intersection between mathematics, physics, biology, chemistry, engineering, and the social sciences. Control of complex networks and complex systems is particularly important since together they comprise most of the world we live in [43]. However, progress in this direction has been particularly challenging due to both the structural complexity of typical networks and the tendency for dynamical processes to be nonlinear. Recent work has made significant progress and shed light on the structural aspects of controllability using the paradigm of linear dynamical systems [11, 12], however, while dynamical systems may display linear dynamics locally, control trajectories, i.e., trajectories leading from undesirable states to desired states, are typically nonlocal [22]. Thus, the design and implementation of efficient and effective control mechanisms for certain applications and classes of problems will likely depend sensitively on particular structural configurations, nonlinear dynamical properties, and specific practical constraints.

In this Article we have focused on the control of synchronization in coupled oscillator networks. Synchronization is a phenomenon vital to many processes that occur in both natural and man-

made systems, including healthy cardiac behavior [44], functionality of cell circuits [45], stability of pedestrian bridges [46], and efficient power grid networks [47]. Specifically we have considered the dynamics network-coupled Kuramoto oscillators [31]—a family of complex systems that importantly incorporates dynamical nonlinearity, dynamical heterogeneity, and structural heterogeneity. We have developed a method for control based on stabilizing the synchronized state via spectral properties of the Jacobian matrix and demonstrated its effectiveness on both Erdős-Rényi and scale-free networks. We observe that driver nodes, i.e., oscillators that require control, tend to balance (in absolute value) large natural frequencies with small degrees. Furthermore, the overall amount of control required to achieve synchronization decreases with both coupling strength and mean degree, while structural heterogeneity tends to have a relatively small effect on the amount of control required.

Finally, we consider direction for potential applications and future directions of research. Recently it was proven that the dynamics of microgrids—a class of small, efficient power networks—are equivalent to Kuramoto oscillators networks [30], making our control mechanism readily applicable to certain power grid problems. Another potential application area lies in cardiac physiology and treatments of cardiac arrhythmia, specifically exploring robust control mechanisms with minimal shock to knock out fatal asynchronous behavior such as cardiac fibrillation [49]. Finally, with our rapidly expanding knowledge of neuroscience comes important questions such as how can we promote normal brain oscillations [50] while repressing disorders such as Parkinson’s disease which are associated with abnormal oscillations [51].

Methods

Steady state solution

To derive the steady state solution $\theta^* = K^{-1}L^\dagger\omega$, we begin with Equation (1). First we note that the mean frequency of all oscillators is given by the mean natural frequency $\langle\omega\rangle$. For simplicity we enter the rotating frame $\theta \mapsto \theta + \langle\omega\rangle t$, effectively setting the mean frequency to zero. Specifically, we are searching for synchronized solutions that typically display a strong degree of phase synchronization, i.e., $r \approx 1$, which is equivalent to considering solutions that satisfy $|\theta_j - \theta_i| \ll 1$ for any pair of network neighbors i and j . In this regime Equation (1) can be linearized to

$$\dot{\theta}_i \approx \omega_i - K \sum_{j=1}^N L_{ij}\theta_j, \tag{4}$$

or equivalently in vector form,

$$\dot{\theta} \approx \omega - KL\theta, \tag{5}$$

where L is the network Laplacian whose entries are defined $L_{ij} = \delta_{ij} \sum_l A_{il} - A_{ij}$. While L has a zero eigenvalue, denoted $\lambda_1 = 0$, rendering it non-invertible, it does have a pseudo-inverse defined using its other eigenvalues (which are non-zero provided that the network is connect) and corresponding eigenvectors, $L^\dagger = \sum_{j=2}^N \lambda_j^{-1} \mathbf{v}^j \mathbf{v}^{jT}$ [39]. Each eigenvector is normalized such that $\{\mathbf{v}^j\}_{j=2}^N$ forms an orthonormal basis for the space of vectors in \mathbb{R}^N with zero mean. Finally, searching Equation (5) for steady-state $\dot{\boldsymbol{\theta}} = \mathbf{0}$ yields the solution $\boldsymbol{\theta}^* = K^{-1} L^\dagger \boldsymbol{\omega}$, as desired.

Gershgorin circle theorem

Definition. (*Gershgorin Discs*) Let M be an $N \times N$ complex matrix. For $i = 1, \dots, N$ let $R_i = \sum_{j \neq i} |M_{ij}|$ be the sum of absolute values of non-diagonal elements of row i , and define $D(M_{ii}, R_i)$ closed disc of radius R_i centered at M_{ii} . $D_i = D(M_{ii}, R_i)$ is the i^{th} Gershgorin Disc.

Theorem. (*Gershgorin*) All eigenvalues of the matrix M lie within the union $\cup_{i=1}^N D_i$ of Gershgorin discs.

References

- [1] Strogatz, S. H. Exploring complex networks. *Nature* **410**, 268–276 (2001).
- [2] Newman, M. E. J. The structure and function of complex networks. *SIAM Rev.* **45**, 167–256 (2003).
- [3] Boccaletti, S., Latora, V., Moreno, Y., Chavez, M. & Hwang, D.–U. Complex networks: structure and dynamics. *Phys. Rep.* **424**, 175–308 (2006).
- [4] Buldyrev, S. V., Parshani, R., Paul, G., Stanley, H. E. & Havlin, S. Catastrophic cascade failures in interdependent networks. *Nature* **464**, 1025–1028 (2010).
- [5] Motter, A. E., Myers, S. A., Anghel, M. & Nishikawa, T. Spontaneous synchrony in power grid networks. *Nature Phys.* **9**, 191–197 (2013).
- [6] Pace, M. L., Cole, J. J., Carpenter, S. R. & Kitchell, J. F. Trophic cascades revealed in diverse ecosystems. *Trens Ecol. Evol.* **14**, 483–488 (1999).
- [7] Scheffer, M., Carpenter, S., Foley, J. A., Folke, C. & Walker, B. Catastrophic shifts in ecosystems. *Nature* **413**, 591–596 (2001).
- [8] May, R. M., Levin, S. A. & Sugihara, G. Complex systems: ecology for bankers. *Nature* **451**, 893–895 (2008).
- [9] Haldane, A. G. & May, R. M. Systemic risk in banking ecosystems. *Nature* **469**, 351–355 (2011).

- [10] Slotine, J.-J. & Li, W. *Applied Nonlinear Control* (Prentice-Hall,1991).
- [11] Liu, Y.-Y., Slotine, J.-J. & Barabási, A.-L. Controllability of complex networks. *Nature* **473**, 167–176 (2011).
- [12] Yuan, Z., Zhao, C., Di, Z., Wang, W.-X. & Lai, Y.-C. Exact controllability of complex networks. *Nat. Commun.* **4**, 2447 (2013).
- [13] Liu, Y.-Y., Slotine, J.-J. & Barabási, A.-L. Control centrality and hierarchical structure in complex networks. *PLoS ONE* **7**, e444459 (2012).
- [14] Yan, G., Lai, Y.-C., Lai, C.-H. & Li, B. Controlling complex networks: How much energy is needed? *Phys. Rev. Lett.* **108**, 218703 (2012).
- [15] Pósfai, M., Liu, Y.-Y., Slotine, J.-J. & Barabási, A.-L. Effect of correlations on network controllability. *Sci. Rep.* **3**, 1067 (2013).
- [16] Jia, T., Liu, Y.-Y., Csóka, E., Pósfai, M., Slotine, J.-J. & Barabási, A.-L. Emergence of bimodality in controlling complex networks. *Nat. Commun.* **4**, 2002 (2013).
- [17] Sun, J. & Motter, A. E. Controllability transition and nonlocality in network control. *Phys. Rev. Lett.* **110**, 208701 (2013).
- [18] Menichetti, G. Dall’Asta, L. & Bianconi, G. Network controllability is determined by the density of low in-degree and out-degree nodes. *Phys. Rev. Lett.* **113**, 078701 (2014).
- [19] Gao, J., Liu, Y.-Y., D’Souza, R. M. & Barabási, A.-L. Target control of complex networks. *Nat. Commun.* **5**, 5415 (2014).
- [20] Nepusz, T. & Vicsek, T. Controlling edge dynamics in complex networks. *Nature Phys.* **8**, 568–573 (2012).
- [21] Sahasrabudhe, S. & Motter, A. E. Rescuing ecosystems from extinction cascades through compensatory perturbations. *Nat. Commun.* **2**, 170 (2011).
- [22] Cornelius, S. P., Kath, W. L. & Motter, A. E. Realistic control of network dynamics. *Nat. Commun.* **4**, 1942 (2013).
- [23] Grigoriev, R. O., Cross, M. C. & Schuster, H. G. Pinning control of spatiotemporal chaos. *Phys. Rev. Lett.* **79**, 2795–2798 (1997).
- [24] Wang, X. F. & Chen, G. Pinning control of scale-free dynamical networks. *Phys. A* **310**, 521–531 (2002).

- [25] Li, X., Wang, X. & Chen, G. Pinning a complex dynamical network to its equilibrium. *IEEE Trans. Circuits Syst., I: Fundam. Theory Appl.* **51**, 2074–2087 (2004).
- [26] Karma, A. Physics of cardiac arrhythmogenesis. *Annu. Rev. Condens. Matter Phys.* **4**, 313–337 (2013).
- [27] Schnitzler, A. & Gross, J. Normal and pathological oscillatory communication in the brain. *Nat. Rev. Neurosci.* **6**, 285–296 (2005).
- [28] Rohden, M., Sorge, A., Timme, M. & Witthaut, D. Self-organized synchronization in decentralized power grids. *Phys. Rev. Lett.* **109**, 064101 (2012).
- [29] Dörfler, F., Chertkov, M., & Bullo, F. Synchronization in complex oscillator networks and smart grids. *Proc. Natl. Acad. Sci. U.S.A.* **110**, 2005–2010 (2013).
- [30] Simpson-Porco, J. W., Dörfler, F. & Bullo, F. Synchronization and power sharing for droop-controlled inverters in islanded microgrids. *Automatica*, **49**, 2603–2611 (2013).
- [31] Kuramoto, Y. *Chemical Oscillations, Waves, and Turbulence* (Springer, New York, 1984).
- [32] Arenas, A., Díaz-Guilera, A., Kurths, J., Moreno, Y. & Zhou, C. Synchronization in complex networks. *Phys. Rep.* **469**, 93–153 (2008).
- [33] Dörfler, F. & Bullo, F. Synchronization in complex networks of phase oscillators: A survey. *Automatica* **50**, 1539–1564 (2014).
- [34] Strogatz, S. H. *Sync: the Emerging Science of Spontaneous Order* (Hyperion, 2003).
- [35] Ott, E. & Antonsen, T. M. Low dimensional behavior of large systems of globally coupled oscillators. *Chaos* **18**, 037113 (2008).
- [36] Lee, W. S., Ott, E. & Antonsen, T. M. Large coupled oscillator systems with heterogeneous interaction delays. *Phys. Rev. Lett.* **103**, 044101 (2009).
- [37] Skardal, P. S. & Restrepo, J. G. Hierarchical synchrony of phase oscillators in modular networks. *Phys. Rev. E* **85**, 016208 (2012).
- [38] Skardal, P. S., Taylor, D. & Sun, J. Optimal synchronization of complex networks. *Phys. Rev. Lett.* **113**, 144101 (2014).
- [39] Ben-Israel, A. & Grenville, T. N. E. *Generalized Inverses* (Springer, New York, 1974).
- [40] Golub, G. H. & Van Loan, C. F. *Matrix Computations* (Johns Hopkins University Press, Baltimore, 1996).

- [41] Erdős, P. & Rényi, A. On the evolution of random graphs. *Publ. Math. Inst. Hung. Acad. Sci.* **5**, 17–61 (1960).
- [42] Molloy, M. & Reed, B. A critical point for random graphs with a given degree sequence. *Random Struct. Algor.* **6**, 161–180 (1995).
- [43] Meyn, S. P. *Control Techniques for Complex Networks* (Cambridge Univ. Press, 2008).
- [44] Karma, A. & Gilmore, R. F. Nonlinear dynamics of heart rhythm disorders. *Phys. Today* **60**, 51–57 (2007).
- [45] Prindle, A., Samayoa, P., Razinkov, I., Danino, T., Tsimring, L. S. & Hasty, J. A sensing array of radically coupled generic ‘biopixels’. *Nature* **481**, 39–44 (2011).
- [46] Strogatz, S. H., Abrams, D. M., McRobie, A., Eckhardt, B. & Ott, E. Theoretical mechanics: Crowd synchrony on the Millennium Bridge. *Nature* **438**, 43–44 (2005).
- [47] Dörfler, F. & Bullo, F. Synchronization and transient stability in power networks and nonuniform Kuramoto oscillators. *SIAM J. Control Optim.* **50**, 1616–1642 (2012).
- [48] Gellings, C. W. & Yeagee, K. E. Transforming the electric infrastructure. *Phys. Today* **57**, 45–51 (2004).
- [49] S. Luther et al. Low-energy control of electrical turbulence in the heart. *Nature* **475**, 235–239 (2011).
- [50] Gross, J., Schmitz, F., Schnitzler, I., Kessler, K., Shapiro, K., Hommel, B. & Schnitzler, A. Modulation of long-range neural synchrony reflects temporal limitations of visual attention in humans. *Proc. Natl. Acad. Sci. U.S.A.* **101**, 13050–13055 (2004).
- [51] Hammond, C., Bergman, H. & Brown, P. Pathological synchronization in Parkinson’s disease: networks, models and treatments. *Trends Neurosci.* **30**, 357–364 (2007).